ISSN 1674-1056
http://cpb.iphy.ac.cn
http://iopscience.iop.org/cpb
中国物理 B
Chinese Physics
中国物理
Chinese Physics B

Phase transition of a diblock copolymer and homopolymer hybrid system induced by different properties of nanorods

Xiao-bo Geng(耿晓波), Jun-xing Pan(潘俊星), Jin-jun Zhang(张进军), Min-na Sun(孙敏娜), Jian-yong Cen(岑建勇)
Citation: Chin. Phys. B . 2018, 27(5): 058102. **doi:** 10.1088/1674-1056/27/5/058102

Journal homepage: http://cpb.iphy.ac.cn; http://iopscience.iop.org/cpb

What follows is a list of articles you may be interested in

Improving self-assembly quality of colloidal crystal guided by statistical design of experiments

Yizhi Wu(吴以治), Xiaoliang Xu(许小亮), Haiming Zhang(张海明), Ling Liu(刘玲), Jichao Li(李继超), Dabao Yang(杨大宝)
Chin. Phys. B . 2017, 26(3): 038105. **doi:** 10.1088/1674-1056/26/3/038105

Controllable preparation of tungsten/tungsten carbide nanowires or nanodots in nanostructured carbon with hollow macroporous core/mesoporous shell

Xiao-Na Ren(任晓娜), Min Xia(夏敏), Qing-Zhi Yan(燕青芝), Chang-Chun Ge(葛昌纯)
Chin. Phys. B . 2017, 26(3): 038103. **doi:** 10.1088/1674-1056/26/3/038103

Dynamics of two polarized nanoparticles

Duan Xiao-Yong, Wang Zhi-Guo
Chin. Phys. B . 2015, 24(11): 118106. **doi:** 10.1088/1674-1056/24/11/118106

From self-assembly to quantum guiding：A review of magnetic atomic structures on noble metal surfaces

Cao Rong-Xing, Zhang Xiao-Pu, Miao Bing-Feng, Sun Liang, Wu Di, You Biao, Ding Hai-Feng
Chin. Phys. B . 2014, 23(3): 038102. **doi:** 10.1088/1674-1056/23/3/038102

Controllable growth of low-dimensional nanostructures on well-defined surfaces

Qin Zhi-Hui
Chin. Phys. B . 2013, 22(9): 098108. **doi:** 10.1088/1674-1056/22/09/098108

Phase transition of a diblock copolymer and homopolymer hybrid system induced by different properties of nanorods*

Xiao-bo Geng(耿晓波)[2], Jun-xing Pan(潘俊星)[1,†], Jin-jun Zhang(张进军)[1,‡], Min-na Sun(孙敏娜)[2], and Jian-yong Cen(岑建勇)[1]

[1] *School of Physics and Information Engineering, Shanxi Normal University, Linfen* 041004, *China*
[2] *School of Chemistry and Materials Science, Shanxi Normal University, Linfen* 041004, *China*

(Received 14 October 2017; revised manuscript received 11 February 2018; published online 26 April 2018)

We investigated phase transitions in a diblock copolymer–homopolymer hybrid system blended with nanorods (NRs) by using the time-dependent Ginzburg–Landau theory. We systematically studied the effects of the number, length and infiltration properties of the NRs on the self-assembly of the composites and the phase transitions occurring in the material. An analysis of the phase diagram was carried out to obtain the formation conditions of sea island structure nanorod-based aggregate, sea island structure nanorod-based dispersion, lamellar structure nanorod-based multilayer arrangement and nanowire structure. Further analysis of the evolution of the domain sizes and the distribution of the nanorod angle microphase structure was performed. Our simulation provides theoretical guidance for the preparation of ordered nanowire structures and a reference to improve the function of a polymer nanocomposite material.

Keywords: self-assembly, block copolymer, nanowires

PACS: 81.16.Dn, 82.35.Jk, 81.07.Gf **DOI:** 10.1088/1674-1056/27/5/058102

1. Introduction

Polymer nanocomposites play a significant technological role in functional materials because of their excellent performance in optical and electronic devices.[1–8] The most promising research subject in polymer nanocomposites is the preparation of highly ordered and controllable nanostructures.[9–11] However, controlling morphology with minimal effort in materials processing remains a considerable challenge. Since the morphology of polymer blends is one of the factors that determines their properties, studying its control is a significant subject in polymer nanocomposite research. For many practical applications, the addition of nanoparticles has been considered as an effective route to material improvement and an important method for creating highly ordered structures.[12–16] In particular, the addition of anisotropic nanoparticles (such as nanorods) to polymeric materials can be beneficial and increase their photoelectric characteristics, optical properties and mechanical properties.[17–23] The nanorods of noble metals (such as gold) and semiconductors (such as CdSe) possess interesting photoelectrical properties and can significantly improve the efficiency of polymer photovoltaic devices by enhancing their carrier mobilities.[24]

In addition, the alignment of nanorods and nanowires plays an important role in determining the electrical conductivity of polymer nanocomposites.[25–28] Therefore, studying how the self-assembly of nanorods into ordered arrays can be facilitated is an important area in nanotechnology. In an early theoretical study, Balazs *et al*. used a coarse-grained model for simulating the self-assembly of binary nanorods.[29] The results showed that when the nanorods have an affinity for one polymer, a component can seed the formation of needle-like percolating networks. Ma *et al*. studied the self-assembly of nanorods in a binary mixture[30] and a diblock copolymer[31] by using a computer simulation method. Their works discussed the influence of the rod–rod interaction, the wetting strength and the rod number density on the architecture and obtained a highly ordered structure of nanowires. Zhang *et al*. used the self-consistent field (SCF) theory to study the phase behavior in mixtures involving cylindrical diblock copolymers and rigid nanorods.[32] Their results indicated that the novel morphologies of the mixtures clearly depended not only on the properties of the polymers but also on the number, length and surface adsorption (neutral, A and B attractive) of the nanorods. The results of this simulation study provide a theoretical guidance for the preparation of polymer nanocomposites. In addition to theoretical investigations, attention has been paid to experimental studies involving blends of nanorods in a polymer system. In recent years, Xu *et al*. showed that controlling the alignment of nanorods within BCP microdomains can be achieved by modifying the chemical properties and supramolecular morphology of the nanorods.[33] Wu and Lu[34] observed an arrangement of silver nanorods in thin films of immiscible polymer

*Project supported by the National Natural Science Foundation of China (Grant No. 21373131), the Provincial Natural Science Foundation of Shanxi, China (Grant No. 2015011004), and the Research Foundation for Excellent Talents of Shanxi Provincial Department of Human Resources and Social Security, China.

†Corresponding author. E-mail: panjunxing2007@163.com
‡Corresponding author. E-mail: zhangjinjun@sxun.edu.cn

© 2018 Chinese Physical Society and IOP Publishing Ltd

blends, which confirmed the theoretical study of Balazs *et al*. These findings can facilitate the fabrication of electrical and optical nanodevices. Experiments by Modestino demonstrated different self-assembly behaviors and vertically aligned CdSe nanorod arrays in polymer composites that can be obtained by controlling the interactions between the nanorod surfaces.[35] Jiang *et al*. studied the effects of gold nanorods (AuNRs) dispersed in homopolymer (P2VP) films. Their experimental results showed that the optical properties of a polymer nanocomposite can be adjusted by changing the volume fraction of the nanorods and the interaction distance between the individual rods.[36] Rasin *et al*. also experimentally examined the impacts of grafted gold nanorods (P2VP-AuNRs) on PS-b-P2VP thin films.[37] Their results showed the dispersion and alignment of AuNRs in a block copolymer thin film at sufficiently low concentrations, which have been validated by the polymer nanocomposite field theory. Meanwhile, there are many experimental[38–45] and theoretical studies[46–62] on the morphologies and phase behaviors of the block copolymer–nanorod system. Moreover, the bridging polymerization in the homopolymer solution in the presence of different interfacial attractions of polymer–particles has also been investigated in some studies.[63,64] As mentioned above, many research efforts have concentrated on the self-assembly of a block copolymer system. In addition, the self-assembly of mixtures of block copolymers and homopolymers in solvents has also been studied. The blend of C homopolymers and AB diblock copolymers can be shown to not only change the volume fraction of blocks in a facile way but also enrich the particle's morphology. Using a simulated annealing method, Kong *et al*. studied the self-assembly of the blends of AB diblock copolymers and C homopolymers in a soft confinement. They discussed the effects of the confinement size, the volume fraction of polymer blocks, the selectivity of the confinement's surface and the incompatibility between blocks on the self-assembly behavior of such systems. They obtained a variety of structures such as pupa-like, pine-cone-like, stacked disks and stacked lamellae. Their results were in accordance with the experiments.[65]

Inspired by these studies, we used cell dynamics simulation (CDS) to study phase transitions in a symmetric diblock copolymer–homopolymer hybrid system induced by nanorods with different properties and found many novel self-assembled structures. The CDS method was originally proposed in a series of work by Oono *et al*. to simulate the interfacial dynamics in the phase separation system. The characteristic of this method is that it quickly simulates the very complex dynamical behavior in large size phase separation systems and can predict new kinetic pathways. The CDS method has been widely used in many fields since it was put forward, for example, CDS studies of self-assembling phase behavior in diblock copolymers/diblock copolymer–homopolymer,[66–74] rock growth,[75,76] polymer crystallization [77,78] and polymer-dispersed liquid crystal.[79] The paper is organized as follows. In Section 2, we detail the computational methodologies employed in this study. The results and relevant discussion are presented in Section 3. The conclusions are drawn in the final section.

2. Model and simulation method

To investigate the phase behavior of the mobile nanorods in a diblock copolymer–homopolymer hybrid system, we used a hybrid method of the Cahn–Hilliard (CH)/Brownian dynamics (BD) model, which has been extensively used by some researchers.[80–82] In this method, for the diblock copolymer–homopolymer hybrid system, we adopted the CH model. For the system of nanorods, we adopted the BD model. For the diblock copolymer–homopolymer hybrid system, its kinetic equation is highly complicated and its specific expression is as follows:

$$\partial\eta/\partial t = M_\eta \nabla^2 \delta F/\delta\eta, \tag{1}$$

$$\partial\psi/\partial t = M_\psi \nabla^2 \delta F/\delta\psi. \tag{2}$$

For the immiscible mixture of diblock copolymer and homopolymer, the volume fractions of the two components satisfy the relation $\phi_A + \phi_B + \phi_C =$ constant, and the two volume fractions are independent. For convenience, one takes $\phi = \phi_A + \phi_B$ and $\psi = \phi_A - \phi_B$ as the independent variables. The variable ϕ is useful to describe the segregation of copolymers and homopolymers, while ϕ plays the role of an order parameter in the microphase separation. Furthermore, we use order parameter $\eta = \phi_A + \phi_B - \psi_c$ instead of ϕ, where ψ_c is the critical composition in the phase diagram for the phase separation between the hompolymer C and diblock copolymer AB, and it depends on the degree of polymerization of each component $\psi_c = \frac{\sqrt{N_C}}{\sqrt{N_{AB}}+\sqrt{N_C}}$, with $N_{AB} = N_A + N_B$. For $\eta > 0$, the volume fraction of the AB component is larger than ψ_c, and the AB diblock copolymer preferentially precipitates from the mixtures. Whereas for $\eta < 0$, homopolymer C precipitates preferentially. The flux of ψ is proportional to the local gradient of the chemical potential, which in turn is proportional to the derivative of the free energy F. In Eqs. (1) and (2), M_η and M_ψ represent the polymer motion and rotation mobility coefficients, respectively, and each nanorod has a center-of-mass position $\boldsymbol{r}_i$ and an orientation angle θ_i as measured from a fixed direction. The variables $\boldsymbol{r}_i$ and θ_i for the i-th rod obey the following Langevin equations:

$$\partial \boldsymbol{r}_i/\mathrm{d}t = -M_1 \partial F/\partial \boldsymbol{r}_i + \eta_i, \tag{3}$$

$$\partial \theta_i/\mathrm{d}t = -M_2 \partial F/\partial \theta_i + \xi_i, \tag{4}$$

where M_1 and M_2 are the mobility coefficients relating to the motion and rotation of the nanorods, and η_i and ξ_i are thermal fluctuations that satisfy the fluctuation–dissipation relations. Equations (3) and (4) are discretized and numerically integrated on a 256 × 256 square lattice, which has periodic boundary conditions in both the x and y directions. The lattice sets the units of length.

The free energy F is composed of three parts $F = F_{\rm GL} + F_{\rm CPL} + F_{\rm RR}$. The free energy of a homopolymer/diblock copolymer is denoted by the Ginzburg–Landau free energy

$$\begin{aligned} & F_{\rm GL}(\eta,\psi) \\ = & \int {\rm d}\boldsymbol{r}\Big\{\Big[-\frac{a}{2}\psi^2+\frac{b}{4}\psi^4+\frac{c}{2}(\nabla\psi)^2\Big] \\ & +\Big[-\frac{a'}{2}\eta^2+\frac{b'}{4}\eta^4+\frac{c'}{2}(\nabla\eta)^2\Big]+b_1\eta\psi-\frac{1}{2}b_2\eta\psi^2\Big\} \\ & +\frac{\alpha}{2}\int\int {\rm d}\boldsymbol{r}{\rm d}\boldsymbol{r}' G(\boldsymbol{r},\boldsymbol{r}')[\psi(\boldsymbol{r})-\psi_0][\psi(\boldsymbol{r}')-\psi_0], \end{aligned} \tag{5}$$

where a, b, c, a', b', c', b_1, and b_2 are all constants. The constant b_1 reflects the interaction comparison between monomers C with both A and B and expressed as[83,84] $b_1 = (-\chi_{\rm AC}+\chi_{\rm BC})/2$. It is now clear that the b_1 term mainly originates from the interaction between the A-B copolymer and the C monomer. If the repulsive interaction strength $\chi_{\rm BC}$ between B and C is large enough, b_1 is positive. The constant b_2 reflects the relationship between C and degree of polymerization N and is given by[85] $b_2 = \frac{1}{\psi_{\rm c}^2 N_{\rm A}}$. The b_2 term represents the fact that the microphase separation should occur only in the copolymer-rich phase. The cross terms (terms with b_1 and b_2) reflect the competition of phase separation between C and A/B. We use N_i (i = A, B, or C) to denote the polymerization degrees of different components. In this section, we set $N_{\rm A} = N_{\rm B}$. The last term on the right corresponds to the long-range correlation, which reflects the microphase separation of the diblock copolymer. $G(\boldsymbol{r},\boldsymbol{r}_0)$ is the Green's function defined by the equation $-\nabla^2 G(\boldsymbol{r},\boldsymbol{r}') = \delta(\boldsymbol{r}-\boldsymbol{r}_0)$, while ψ_0 is the spatial average of ψ. Here, we set $\psi_0 = 0$ for the case of a symmetric diblock copolymer. α is a parameter that describes the strength of the long-range force owing to the covalent linkage between the A and B components.[86–88]

The $F_{\rm CPL}$ describes the interactions between the nanorods and the polymer, and is given by

$$\begin{aligned} F_{\rm CPL} = & \int {\rm d}\boldsymbol{r}\sum_i\int {\rm d}\boldsymbol{s}_i\int {\rm d}\boldsymbol{s}_i V_0 \\ & \times\exp\left(\frac{-|\boldsymbol{r}-\boldsymbol{s}_i|}{r_0}\right)(W(\boldsymbol{r})-W_\omega)^2, \end{aligned} \tag{6}$$

where $\boldsymbol{s}_i = \boldsymbol{r}_i + \delta\boldsymbol{s}_i$ indicates a point on the surface of the nanorods, and $\int {\rm d}\boldsymbol{r}_i$ represents the integral over the length of the i-th nanorod. When $W = \psi = \phi_{\rm A}+\phi_{\rm B}$ and $W_\omega = \psi_\omega = 1$, the nanorods are preferentially wetted the A phase. When $W = \psi = \phi_{\rm A}+\phi_{\rm B}$ and $W_\omega = \psi_\omega = -1$, the nanorods are preferentially wetted the B phase. When $W = \eta_w = \phi_{\rm A}+\phi_{\rm B}-\psi_{\rm c}$ and $W_\omega = \eta_\omega = -1$, the nanorods are preferentially wetted in the C phase. We assume the short-ranged wetting interaction $V(\boldsymbol{r}-\boldsymbol{s}_i) = V_0\exp(-|\boldsymbol{r}-\boldsymbol{s}_i|/r_0)$, where V_0 (>0) is the wetting strength parameter that represents the short-range interactions between the nanorods and the polymer component. r_0 indicates the range of the interactions and can be tuned by varying the chemical nature and length of the chains coated on the rods.

The $F_{\rm RR}$ represents the interactions of the nanorods. In this paper, we assume that pure repulsion is dependent on the distance and angle between the pairs of rods i and j

$$F_{\rm RR} = \begin{cases} \chi\sum\limits_i\sum\limits_j(L-|\boldsymbol{r}_i-\boldsymbol{r}_j|^2) \\ \times\left[4/3-\cos^2(\theta_i-\theta_j)\right], & \text{if } |\boldsymbol{r}_i-\boldsymbol{r}_j|<L, \\ 0, & \text{if } |\boldsymbol{r}_i-\boldsymbol{r}_j|\geq L, \end{cases} \tag{7}$$

where χ represents the intensity of the nanorods interactions and L represents the length of the nanorods. This interaction leads to an isotropic–nematic ordering for the pure rod system. From this equation, we can see that the interaction between the rods strongly depends on these two parameters. When χ is fixed, the smaller L is, the weaker the repulsion is; and the larger L is, the stronger repulsion is. Next we adopted the method of CDS,[89–92] where the dynamic equations (1)–(7) were used in a 256×256 two-dimensional space with discretization and periodic boundary conditions. In the following simulations, the parameters are set as $M_\psi = M_\eta = 1.0$, $M_1 = 1.0$, $M_2 = 0.1$, $b_1 = 0.1$, $b_2 = 0.2$, $\alpha = 0.02$, $\chi = 0.6$, $r_0 = 3.0$, $V_0 = 0.04$, $N_{\rm A} = N_{\rm B} = 24$, $N_{\rm C} = 34$, $\Delta t = 0.5$. The above parameter setting is the experience values selected from the previous researchers' work. In this paper, all variables have been rescaled into dimensionless units.

3. Numerical results and discussion

Figure 1(a) shows a late-stage snapshot of the phase separation occurring in a pure symmetric diblock copolymer–homopolymer hybrid system in the absence of the nanorods. The red regions relate to phase A, the blue regions to phase B and the green regions to phase C. From Fig. 1(a), it can be deduced that the mixed system of AB/C is formed from a sea-island structure. The self-assembly of nanorods in the absence of diblock copolymer and homopolymer is shown in Fig. 1(b), the nanorods are uniformly dispersed in the lattice and form an isotropic phase.

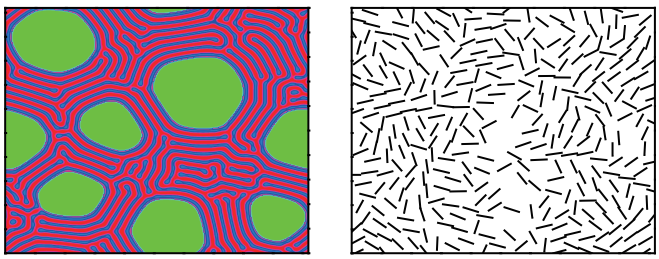


Fig. 1. (color online) (a) Morphology of the self-assembled pure AB diblock copolymer–C homopolymer hybrid system without the nanorods. The red regions are A domains, the blue regions are B domains and the green regions are C domains. (b). Morphology of the self-assembled pure nanorods, with $N_s = 340$, $L = 13$, and AB : C = 70 : 30.

When the nanorods are dispersed into the diblock copolymer–homopolymer hybrid system, the system can self-assemble into phase-rich structures. Figure 2(a) shows the phase diagram involving the C-affinity nanorods for different numbers (N_s) and lengths (L) of the nanorods. Figures 2(b1)–2(b5) show the morphologies of the mixture: (i) a sea-island/nanorod aggregation structure (SI-G, the solid square, Fig. 2(b1)), where the AB/C polymers form a sea-island structure and the nanorods aggregate in the C domain; (ii) a sea island/nanorod dispersion structure (SI-D, the solid circle, Fig. 2(b2)), where the AB/C polymers form a sea island structure and the nanorods disperse in the C domain; (iii) a lamellar/nanorods multilayer arrangement structure (L-MP, the solid triangle, Fig. 2(b3)), where the AB/C polymers form a lamellar structure and the nanorods disperse into the C domain and align in a short end-to-end structure; (iv) a nanowire structure (L-SP, the star, Fig. 2(b4)), where the AB/C polymer form a lamellar structure and the nanorods in the C domain align in an end-to-end structure; and (v) a disordered structure (Dis, the rhombus, Fig. 2(b5)). From the phase diagram, we can see that, for the short nanorods ($3 \leq L \leq 5$), when their number density is in the low range 0.18%–1.7% ($40 \leq N_s \leq 220$), the system can self-assemble into an SI-G structure. When the number of nanorods is increased ($220 < N_s \leq 400$, i.e., the number density is 1.0%–3.1%), the SI-D structures are observed. In case of longer nanorods ($7 \leq L \leq 9$), when their number density is low 0.43%–3.4% ($40 \leq N_s \leq 250$), the system can self-assemble into an SI-D structure. The novel phase morphology (L-MP) structure is observed by increasing the number of nanorods ($250 < N_s \leq 400$, i.e., the number density is 2.7%–5.5%). In case of long nanorods ($11 \leq L \leq 13$), when the number density is low 0.68%–3.2% ($40 \leq N_s \leq 160$), the system can self-assemble into an SI-D structure. When the nanorod number increases ($160 < N_s \leq 400$, i.e., the number density is 2.7%–7.9%), the induced morphological transition of the system follows the trend from SI-D to L-MP and to L-SP. Up to a NR length $L = 15$, for increasing number density ($40 \leq N_s \leq 400$, i.e., the number density is 0.92%–9.2%), the rich morphological transition from SI-D to L-MP to L-SP and to Dis is observed.

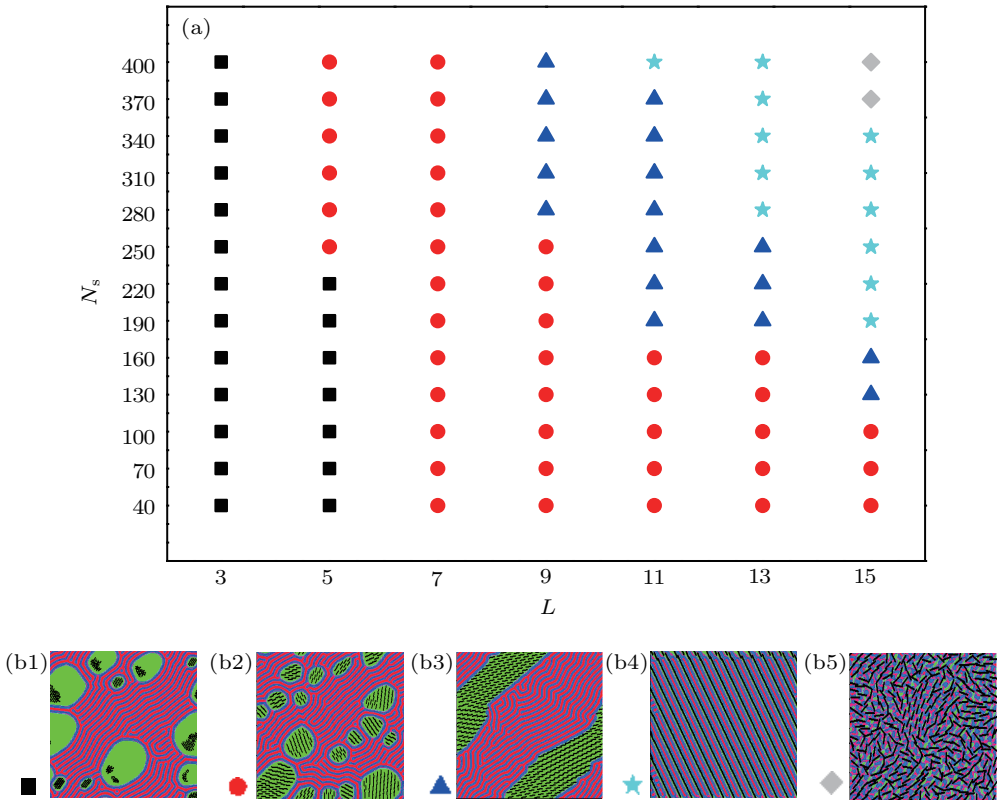


Fig. 2. (color online) Phase diagram for mixtures of the symmetric diblock copolymer–homopolymer hybrid system and NRs with different NR lengths (L) and numbers (N_s). The symbols represent the corresponding morphologies. The red regions are A domains, the blue regions are B domains and the green regions are C domains.

From the phase diagram, we know that when the nanorods are short, they have a slight influence on the polymer system. So the polymer structure is similar to the AB/C bulk sea-island structure without the nanorods. When the length of the nanorods gradually increases, we can obviously see that the added nanorods have an influence on the polymer system and the sea-island structure of the original system is broken. The nanorods in the C domain align in an end-to-end structure, which is greatly influenced by the number of the nanorods. When the nanorods are few ($40 < N_s < 100$), they aggregate in the C domain. When there are some nanorods ($100 \leq N_s < 190$), the nanorods disperse in the C domain and align end-to-end as a short nanowire. If the number density is small, it cannot form a large-scale nanowire structure. hence, it has a limited effect on the polymer system. When the number of nanorods is greater ($N_s > 190$), the system forms a nanowire structure through the whole range. The phenomenon can be explained as follows. Due to wetting interactions between the nanorods and the polymers, the nanorods are confined in the favorable C domains. When the nanorods are short, the weak repulsive interactions between them cause the rods to aggregate in the C component. As the length of the nanorods increased, the repulsive interactions become more obvious and result in them forming a parallel array of short-range nanowire structures in the C component. As the nanorod length is further increased, the interactions between the rods are enhanced as well, leading to the formation of a long end-to-end aligned nanowire structure throughout the region. Meanwhile, due to the interactions between the polymer components, the AB chains extend perpendicular to the macrophase interfaces that finally result in the formation of the nanowire structure. When the length and number of the nanorods exceed a certain limit, their interactions extend far beyond the constraints imposed by the C component, causing the nanorods to distribute over the whole area and form a disordered structure.

In order to quantitatively investigate the phase behaviors of the nanorods included in the diblock copolymer and homopolymer hybrid system, we numerically calculate the domain size $R(t)$ in the x or y direction as a function of time. This is derived from the inverse of the first moment of the structure factor $S(k,t)$ as $R_i = 2\pi/\langle k_i(t)\rangle$, where $\langle k_i(t)\rangle = \int \mathrm{d}K k_i S(K,t) / \int \mathrm{d}K S(K,t)$. The structure factor $S(K,t)$ is determined by the Fourier component of the spatial concentration distribution. All results are averaged over 10 independent runs. Figure 3 shows the time evolution of the microdomain sizes $R(t)$ in the x and y directions. From Fig. 3, we can see that the domain sizes $R_x(t)$ and $R_y(t)$ are almost the same. We also see that in equilibrium, the nanorod length increases while the microdomain sizes R_x and R_y gradually decrease from curve a to curve e. This indicates that the coarsening of microdomains is suppressed as the nanorods length increases. From the curves in Fig. 3, we can see that in the early stage ($t < 5 \times 10^5$), the microdomain growth is slow and not significantly affected by the change in the nanorod length. In the middle stage ($5 \times 10^5 < t < 2 \times 10^6$), the microdomain size undergoes an obvious change. While it is stable in the later stage ($t > 2 \times 10^6$). From curve e in Fig. 3, we can see that the growth in microdomain size is minimal as the time step is increased.

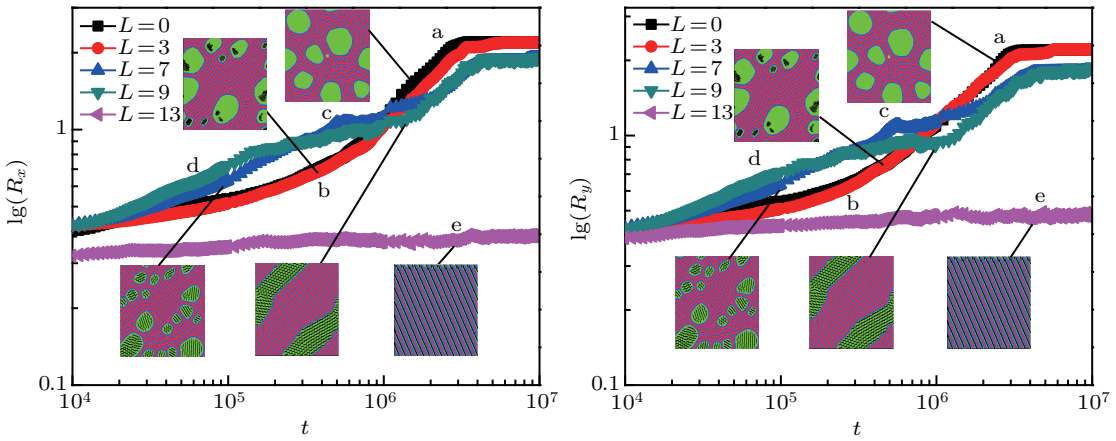


Fig. 3. (color online) The time evolution of the characteristic sizes of microdomains $R_x(t)$ and $R_y(t)$ for different nanorods with nanorods number $N_s = 340$. Curve a, $L = 0$; curve b, $L = 3$; curve c, $L = 7$; curve d, $L = 9$; and curve e, $L = 13$.

Furthermore, in order to explore the process of forming the ordered structure discussed above (Figs. 3(d) and 3(e)), we show the pattern evolution of diblock Copolymer–homopolymer/nanorods when $N_s = 340$, $L = 9$ and $L = 13$ in Fig. 4. From Figs. 4(a1)–4(a3), we can see that in the early stage ($t = 1 \times 10^4$), the system exhibits a disordered structure and the nanorods show a dispersed state, which is due to the interfacial energy between the polymer components dominating the phase separation (Fig. 4(a1)). When $t \geq 1 \times 10^5$, the repulsive interaction of the nanorods and the rod–polymer interaction begin to appear. The dispersed C domains are aggregated due to the synergistic effect of the rod–polymer interaction and

the interfacial energy of the polymer components (Fig. 4(a2)). Later, the system can self-assemble into a lamellar/nanorods multilayer arrangement (L-MP) structure (Fig. 4(a3)). From Figs. 4(b1)–4(b3), we can see that the interactions of the rods and rod–polymer have already played an important role in the beginning of the evolution of the system. At the same time, the repulsive energy between the rods inhibits the phase separation driven by the interfacial energy between the polymer components, making the system form an ordered structure in a short time (Figs. 4(b1)–4(b3)).

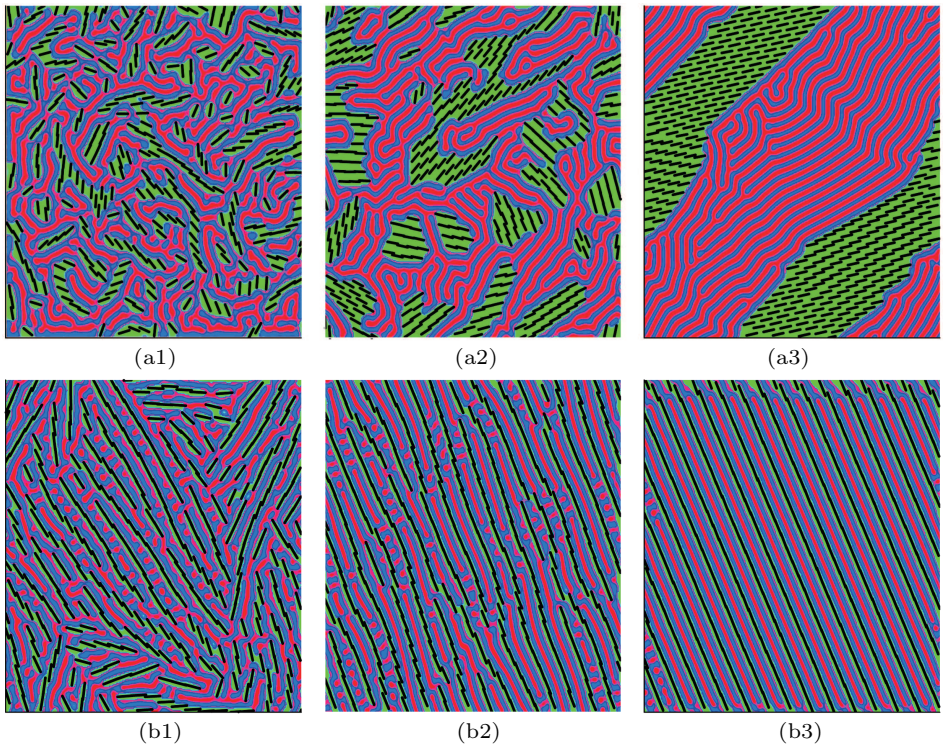


Fig. 4. (color online) The pattern evolution of diblock copolymer–homopolymer/nanorods at different time with $N_s = 340$, (a) $L = 9$ and (b) $L = 13$ correspond to Figs. 3(d) and 3(e). (a1) $t = 1 \times 10^4$, (a2) $t = 1 \times 10^5$, (a3) $t = 5 \times 10^6$, (b1) $t = 1 \times 10^4$, (b2) $t = 1 \times 10^5$, (b3) $t = 5 \times 10^6$. The red regions are A domains, the blue regions are B domains, the green regions are C domains and the nanorods are represented by the black lines.

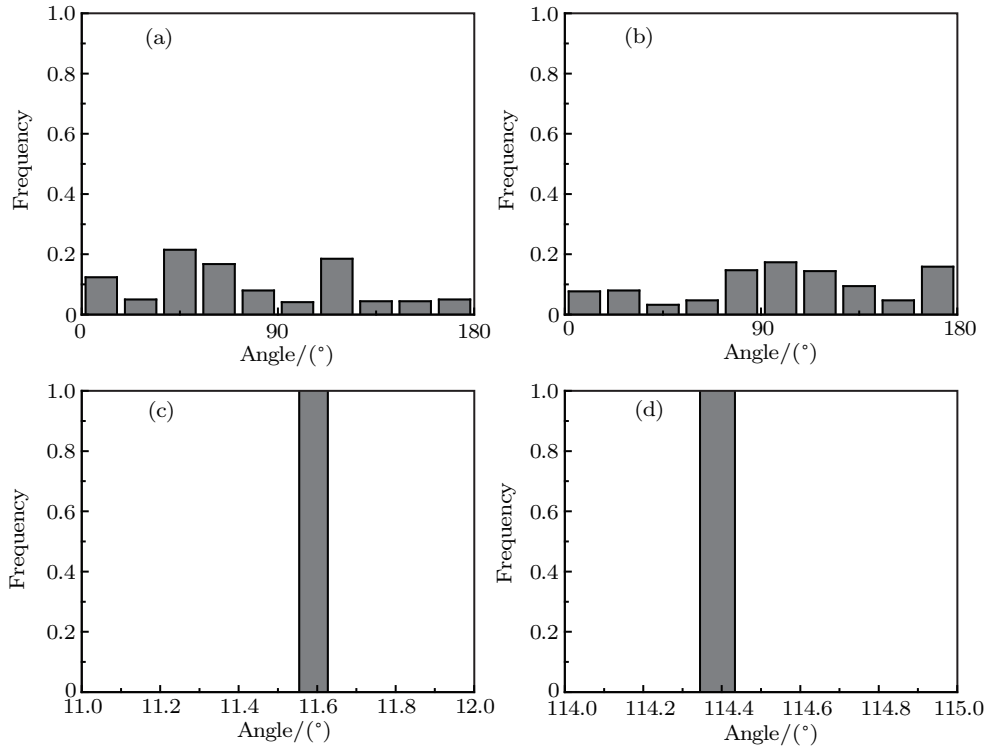


Fig. 5. Angle of nanorods long axis direction and horizontal direction angle corresponding to (a) $N_s = 340$, $L = 3$, (b) $N_s = 340$, $L = 7$, (c) $N_s = 340$, $L = 9$, (d) $N_s = 340$, $L = 13$.

In order to further study the microscopic phase transition in the diblock copolymer–homopolymer system in the presence of nanorods, we show the histograms of the angular distribution of nanorods having different lengths for $N_s = 340$ in Fig. 5, which correspond to Figs. 2(b1)–2(b4). The horizontal coordinate is the angle between the long axis of a nanorod and the horizontal direction. In Figs. 5(a) and 5(b), it can be seen that almost all of the rods orient between 0 to π. The angular distribution of the nanorods is dispersed, which is consistent with the structures revealed in Figs. 2(b1) and 2(b2). This indicates that the nanorods are randomly oriented and isotropic in the island structure. In Fig. 5(c), we know that all angles of the nanorods are 11.6°. Similarly, all angles of the nanorods displayed in Fig. 5(d) are 114.4°. Corresponding to Figs. 2(b3) and 2(b4), the nanorods are directionally distributed and show anisotropy in the layered structure.

In the meantime, we study the effect of the C component polymerization degree (N_C) on the system structure. The results show that the polymerization degree of the C component has little effect on the system structure.

We consider the influence of different infiltration properties on the phase behavior of the system. For the nanorods infiltrating the B component of a diblock copolymer, we construct an approximate phase diagram as a function of their length and number. In the phase diagram shown in Fig. 6, the solid circles and squares represent the ordered and disordered structures, respectively. From the phase diagram, we know that when the number of nanorods $N_s \leq 200$, the resulting system is always a disordered structure. When the number of nanorods is $N_s > 200$ and their lengths are sufficiently long, the system undergoes a transformation from the disordered to the ordered structure.

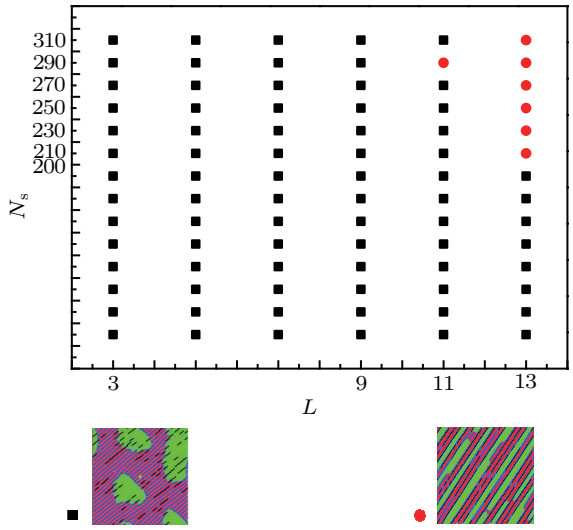


Fig. 6. (color online) The phase diagram of a symmetric diblock copolymer-*homopolymer hybrid system and NR mixtures for different NR lengths L and numbers N_s. Symbols correspond to the morphologies. The phase diagram shows that the nanorods infiltrate the B components. The red regions are A domains, the blue regions are B domains and the green regions are C domains.

We consider the effects of the different infiltration properties on the phase behavior of the system. For the nanorods having an affinity for the A block, we develop a phase diagram as a function of the nanorod number and length. In the phase diagram shown in Fig. 7, the solid circles and squares represent the ordered and disordered structures, respectively. From the phase diagram, we can see that for relatively small ($N_s \leq 200$) nanorod numbers, the systems always form a disordered structure irrespective of the lengths of the nanorods. When the number of nanorods is greater ($N_s \geq 230$), the system forms an ordered structure for large nanorod lengths.

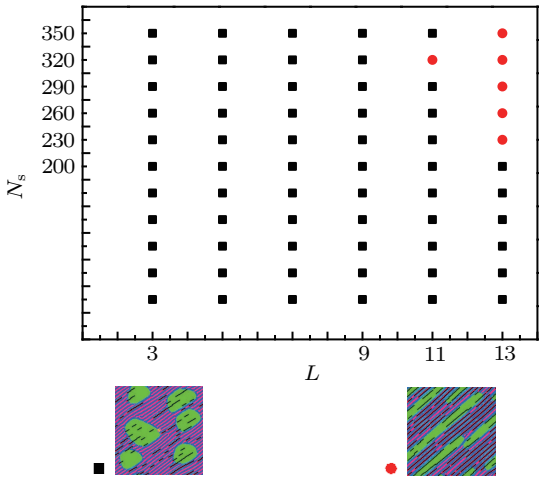


Fig. 7. (color online) The phase diagram for the symmetric diblock copolymer–homopolymer hybrid system and a NR mixture with different NR lengths L and numbers N_s. Graphic symbols correspond to the morphologies. The phase diagram shows that the nanorods infiltrate the A components. The red regions are A domains, the blue regions are B domains, and the green regions are C domains.

4. Conclusion

In summary, we used a computer simulation to study the phase transitions in a diblock copolymer–homopolymer hybrid system blended with nanorods. The results demonstrated that when the nanorods infiltrated the C component, the following system transformations occurred with the increase in the number of nanorods and length: (SI-G) to (SI-D) to (L-MP) to (L-SP) to (DIS). When the nanorods infiltrated the B component, a system transformation from the disordered structure to an ordered structure occurred as the number and length of the nanorods increased. When the nanorods infiltrated the A component, the increase in the number and length of the nanorods caused a system transformation from a disordered structure to an ordered structure. Meanwhile, we analyzed the evolution in pattern and the domain growth of these morphologies and structures. Our simulation provides a theoretical guidance for the preparation of an ordered nanowire structure and serves as a beneficial reference for improving the function of polymer nanocomposites.

References

[1] Kao J, Thorkelsson K, Bai P, Rancatore B J and Xu T 2013 *Chem. Soc. Rev.* **42** 2654
[2] Lin Y, Lim J A, Wei Q, Mannsfeld S C B, Briseno A L and Watkins J J 2012 *Chem. Mater.* **24** 622
[3] Grubbs R B 2005 *Polym. Sci. J. Part A: Polym. Chem.* **43** 4323
[4] Park J H and Joo Y L 2014 *Phys. Chem. Chem. Phys.* **16** 8865
[5] Chen H Y and Ruckenstein E 2010 *Polymer* **51** 5869
[6] Chen H Y and Ruckenstein E 2009 *J. Chem. Phys.* **131** 244904
[7] Liu J, Wang Z X, Zhang Z Y, Shen J X, Chen Y L, Zheng Z J, Zhang L Q and Lyulin A V 2017 *J. Phys. Chem. B* **121** 9311
[8] Chao H, Koski J and Riggleman R A 2017 *Soft Matter* **13** 239
[9] Feng J and Ruckenstein Eli 2007 *J. Chem. Phys.* **126** 124902
[10] Guo H X 2006 *J. Chem. Phys.* **124** 054902
[11] Lisal M and Brennan J K 2007 *Langmuir* **23** 4809
[12] Garcia B C, Kamperman M, Ulrich R, Jain A, Gruner S M and Wiesner U 2009 *Chem. Mater.* **21** 5397
[13] Yeh S W, Wei K H, Sun Y S, Jeng U S and Liang K S 2005 *Macromolecules* **38** 6559
[14] Daga V K, Anderson E R, Gido S P and Watkins J J 2011 *Macromolecules* **44** 6793
[15] Lin Y, Daga V K, Anderson E R, Gido S P and Watkins J J 2011 *J. Am. Chem. Soc.* **133** 6513
[16] Shebert G L and Joo Y L 2016 *Soft Matter* **12** 6132
[17] Guo Y Q, Pan J X, Sun M N and Zhang J J 2017 *J. Chem. Phys.* **146** 024902
[18] Ryan K M, Mastroianni A, Stancil K A, Liu H T and Alivisatos A P 2006 *Nano Lett.* **6** 1479
[19] Hu J T, Li L S, Yang W D, Manna L, Wang L W and Alivisatos A P 2001 *Science* **5524** 2060
[20] Zhang S, Feng Y, Ning N Y, Zhang L Q, Tian M and Mi J G 2017 *Comput. Mater. Sci.* **129** 107
[21] Thorkelsson K, Bronstein N and Xu T 2016 *Macromolecules* **49** 6669
[22] Ting C L, Composto R J and Frischknecht A L 2016 *Macromolecules* **49** 1111
[23] Hore M J A and Composto R J 2013 *Macromolecules* **47** 875
[24] Huynh W U, Dittmer J J and Alivisatos A P 2002 *Science* **5564** 2425
[25] White S I, Mutiso R M, Vora P M, Jahnke D, Hsu S, Kikkawa J M, Li J, Fischer J E and Winey K I 2010 *Adv. Funct. Mater.* **20** 2709
[26] White S I, DiDonna B A, Mu M, Lubensky T C and Winey K I 2009 *Phys. Rev. B* **79** 024301
[27] Mutiso R M, Sherrott M C, Li J and Winey K I 2012 *Phys. Rev. B* **86** 214306
[28] Mutiso R M, Sherrott M C, Rathmell A R, Wiley B J and Winey K I 2013 *ACS Nano* **7** 7654
[29] Peng G, Qiu F, Ginzburg V V, Jasnow D and Balazs A C 2000 *Science* **288** 1802
[30] Chen K and Ma Y Q 2002 *Phys. Rev. E* **65** 041501
[31] Chen K and Ma Y Q 2002 *J. Chem. Phys.* **116** 7783
[32] He Li L, Zhang L X, Chen H P and Liang H J 2009 *Polymer* **50** 3403
[33] Thorkelsson K, Mastroianni A J, Ercius P and Xu T 2011 *Nano Lett.* **12** 498
[34] Wu K H and Lu S Y 2006 *Macromol. Rapid Commun.* **27** 424
[35] Modestino M A, Chan E R, Hexemer A, Urban J J and Segalman R A 2011 *Macromolecules* **44** 7364
[36] Jiang G Q, Hore M J A, Gam S and Composto R J 2012 *ACS Nano* **6** 1578
[37] Rasin B, Chao H K, Jiang G Q, Riggleman R A and Composto R J 2016 *Soft Matter* **12** 2177
[38] Ploshnik E, Salant A, Banin U and Shenhar R 2010 *Adv. Mater.* **22** 2774
[39] Ploshnik E, Salant A, Banin U and Shenhar R 2010 *Phys. Chem. Chem. Phys.* **12** 11885
[40] Deshmukh R D, Liu Y and Composto R J 2007 *Nano Lett.* **7** 3662
[41] Zhang Q L, Gupta S, Emrick T and Russell T P 2006 *J. Am. Chem. Soc.* **128** 3898
[42] Frischknecht A L, Hore M J A, Ford J and Composto R J 2013 *Macromolecules* **46** 2856
[43] Thorkelsson K, Nelson J H, Alivisatos A P and Xu T 2013 *Nano Lett.* **13** 4908
[44] Lai F Y, Borca T T and Plawsky J 2015 *Nanotechnology* **26** 055301
[45] Modestino M A, Chan E R, Hexemer A, Urban J J and Segalman R A 2011 *Macromolecules* **44** 7364
[46] Chakraborty S and Roy S 2015 *J. Phys. Chem. B* **119** 6803
[47] Horsch M A, Zhang Z L and Glotzer S C 2006 *J. Chem. Phys.* **125** 184903
[48] Park J H, Kalra V and Joo Y L 2014 *J. Chem. Phys.* **140** 124903
[49] Chai A H, Zhang D, Jiang Y W, He L L and Zhang L X 2013 *J. Chem. Phys.* **139** 104901
[50] Yang Z, Ping L X and Xuan Z Q 2011 *Polymer* **52** 6110
[51] He L L, Zhang L X, Xia A and Liang H J 2009 *J. Chem. Phys.* **130** 144907
[52] He L L, Zhang L X and Liang H J 2010 *Polymer* **51** 3303
[53] Tang Q and Ma Y Q 2009 *J. Phys. Chem. B* **113** 10117
[54] Zhou Y, Long X. P and Zeng Q X 2011 *Polymer* **26** 6110
[55] Ma X, Yang Y Z, Zhu L, Zhao B, Tang P and Qiu F 2013 *J. Chem. Phys.* **139** 214902
[56] Sides S W, Kim B J, Kramer E J and Frederickson G H 2006 *Phys. Rev. Lett.* **96** 250601
[57] Park J H, Yin J, Kalra V and Joo Y L 2014 *J. Phys. Chem. C* **118** 7653
[58] Wang K, Jin S M, Xu J P, Liang R J, Shezad K, Xue Z G, Xie X L, Lee E and Zhu J T 2016 *ACS Nano* **10** 4954
[59] Cheng M H, Hsu Y C, Chang C W, Ko H W, Chung P Y and Chen J T 2017 *ACS Applied Materials Interfaces* **9** 21010
[60] He L L, Li S B and Zhang L X 2013 *J. Appl. Polym. Sci.* **127** 4470
[61] Chakraborty S and Roy S 2015 *J. Phys. Chem. B* **119** 6803
[62] Li S B, Chen P, Wang X H, Zhang L X and Liang H J 2009 *J. Chem. Phys.* **130** 014902
[63] Hall L M, Jayaraman A and Schweizer K S 2010 *Curr. Opin. Solid State Mater. Sci.* **14** 38
[64] Chen K, Li H S, Zhang B K, Li J and Tian W D 2016 *Sci. Rep.* **6** 20355
[65] Zhang J, Kong W and Duan H 2017 *Langmuir* **33** 3123
[66] Zhang L C, Sun M N, Pan J X, Wang F B, Zhang J J and Wu H S 2013 *Chin. Phys. B* **22** 096401
[67] Pinna M, Zvelindovsky A V, Todd S and Goldbeck W G 2006 *J. Chem. Phys.* **125** 154905
[68] Pinna M and Zvelindovsky A V 2012 *Eur. Phys. J. B* **85** 210
[69] Yan L T, Schoberth H G and Boker A 2009 *Macromol. Chem. Phys.* **210** 1003
[70] Ito A 1998 *Phys. Rev. E* **58** 6158
[71] Ohta T and Ito A 1995 *Phys. Rev. E* **52** 5250
[72] Ren S R, Hamley I W, Teixeira P I C and Olmsted P D 2001 *Phys. Rev. E* **63** 041503
[73] Ohta T and Kawasaki K 1986 *Macromolecules* **19** 2621
[74] Huo Y, Zhang H and Yang Y 2003 *Macromolecules* **36** 5383
[75] Veysey II J, Fouke B W, Kandianis M T, Schickel T J, Johnson R W and Goldenfeld N 2008 *J. Sediment. Res.* **78** 69
[76] Veysey II J and Goldenfeld N 2008 *Nature* **4** 310
[77] Wang D, Shi T, Chen J, An L J and Jia Y X 2008 *Chem. Phys.* **129** 194903
[78] Zhou D, Shi A C and Zhang P 2008 *J. Chem. Phys.* **129** 154901
[79] Teixeira P I C and Mulder B M 1996 *Phys. Rev. E* **53** 1805
[80] Ginzburg V V, Qiu F, Paniconi M, Peng G W, Jasnow D and Balazs A C 1999 *Phys. Rev. Lett.* **82** 4026
[81] Qiu F, Ginzburg V V, Paniconi M, Peng G W, Jasnow D and Balazs A C 1999 *Langmuir* **15** 4952
[82] Buxton G A and Balazs A C 2004 *Mol. Simul.* **30** 249
[83] Ito A 1998 *Phys. Rev. E* **58** 6158
[84] Liu B, Tong C H and Yang Y L 2001 *J. Phys. Chem. B* **105** 10091
[85] Tong C and Yang Y 2002 *J. Chem. Phys.* **116** 1519
[86] Oono Y and Bahiana M 1988 *Phys. Rev. Lett.* **61** 1109
[87] Bates F S and Fredrickson G H 1990 *Annu. Rev. Phys. Chem.* **41** 525
[88] Chakrabarti A and Gunton J D 1993 *Phys. Rev. E* **47** 792
[89] Oono Y and Puri S 1987 *Phys. Rev. Lett.* **58** 836
[90] Puri S and Oono Y 1988 *Phys. Rev. A* **38** 1542
[91] Oono Y and Puri S 1988 *Phys. Rev. A* **38** 434
[92] Bahiana M and Oono Y 1990 *Phys. Rev. A* **41** 6763